Proceedings
of the 4th International Modelica Conference,
Hamburg, March 7-8, 2005,
Gerhard Schmitz (editor)

M. Rubio, A. Urquia, L. González, D. Guinea, S. Dormido
UNED and CSIC, Madrid, Spain
FuelCell Lib - A Modelica Library for Modeling of Fuel Cells
pp. 75-82

*FuelCell*Lib - A Modelica Library for Modeling of Fuel Cells

Miguel A. Rubio[+], Alfonso Urquia*, Leandro González[+], Domingo Guinea[+], Sebastian Dormido*

[+] Instituto de Automática Industrial (IAI), CSIC
Ctra. Campo Real, Km. 0,200 – La Poveda, 28500 Arganda del Rey, Madrid, Spain
E-mail: {marubio, leandrog, domingo}@iai.csic.es

* Departamento de Informática y Automática, E.T.S. de Ingeniería Informática, UNED
Juan del Rosal 16, 28040 Madrid, Spain
E-mail: {aurquia, sdormido}@dia.uned.es

Abstract

The design, implementation and use of *FuelCell*Lib library are discussed. *FuelCell*Lib is a Modelica library for the dynamic modeling of fuel cells (FC). It is intended to be used for: (1) enhancing the understanding of the physical-chemical phenomena involved in the fuel-cell operation; and (2) optimizing the performance of the fuel cells. Physical phenomena are modeled using different hypotheses, in order to allow different levels of detail in the fuel-cell description. *FuelCell*Lib version 1.0 (release on January, 2005) is free software, and it will be available on the website of the Modelica Association.

1   Introduction

During the last decades, the planet has been suffering a serious environmental decay, partially due to the use of fossil fuels. As a consequence, a great effort is being made to find alternative sources of energy. The fuel-cells (abbreviated: FC) constitute an alternative source of energy for automotive and residential use.

The modeling and simulation of the fuel-cells is an active research field. Some existing fuel-cell libraries, developed by otˆ#   authors, have been implemented by using causal simulation languages (for instance, SIMULINK [1]) and fluid-dynamic simulation programs [2]. However, these approaches do not facilitate the modeling task and the model reuse.

The approach adopted in the *FuelCell*Lib implementation is different. In order to facilitate easy upgrade and reuse of the models, it has been designed and programmed following the object-oriented modeling methodology.

*FuelCell*Lib is not the only library for fuel-cell modeling written in Modelica language. The library implemented by Steinmann and Treffinger is presented in [3]. Its models are intended for describing the steady-state behavior of the fuel cells, and they do not take into account the dependence with the spatial coordinate. On the contrary, *FuelCell*Lib models are intended for describing the dynamic behavior, taking into account the spatial coordinate. The *FuelCell*Lib modeling hypothesis are discussed next.

2   Fuel-cell design and operation

The fuel-cell is composed of the following seven fundamental parts: the active layers, the diffusion layers, the terminals of the anode and the cathode, and the membrane (see Fig. 1).

The membrane is placed between the catalytic layers of the anode and the cathode. Protons migrate through the membrane, from the anode to the cathode, along with water. Generally, the proton-exchange membranes are made of Nafion, which guarantees a high protonic conductivity.
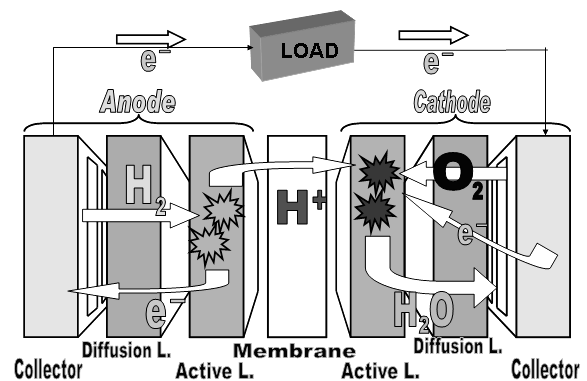

Figure 1: Schematic representation of PEMFC

Usually, the catalyst employed in the active layer is platinum. A small percentage of ruthenium is added, in order to inhibit the poisoning effect of the carbon monoxide. The catalyst is mixed with coal and electrolyte. This catalytic ink is usually deposited over the surface of the anode and cathode diffusion layers.

The diffusion layers are made of porous material to allow the gases and water transport to the catalytic layer. In addition, this diffusion material needs to be a good electric conductor, to allow the flow of electrons between the collector plates and the catalytic layers. The diffusion layer is usually manufactured from coal, paper or cloth. Their conductivity and their resistance to corrosion make these materials adequate.

The collector plates are made of metallic material or non-porous coal. The three fundamental characteristics of these materials are the following: (1) their high electric conductivity; (2) their capacity to maintain a tight cell; and (3) their ability to allow the correct distribution of reagents through the channels.

3   Phenomena modeled

The most outstanding phenomena of PEMFC (i.e., fuel cells with combustible hydrogen) take place in the cell cathode [4,5]. The physical-chemical phenomena modeled in *FuelCell*Lib include the following (see Fig. 2):

Membrane:

-    Transport of water in liquid and steam phase.
-    Protonic conduction.

Catalytic layer of cathode:

-    Transport of water in liquid and steam phase.
-    Transport of oxygen in steam phase.
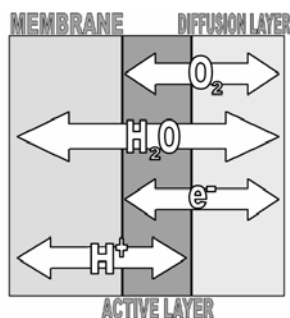-   Protonic and electronic conduction.
-    Electro-catalytic reaction.

Diffusion Layer of cathode:

-    Transport of water in liquid and steam phase.
-    Transport of oxygen in steam phase.
-    Electronic conduction.

Therefore, the *FuelCell*Lib models include the following physical-chemical phenomena: the diffusion of gases in porous media, the electronic and protonic conduction and electrochemical reactions. The method of finite volumes is applied for discretizing the PDE.

In addition, the *FuelCell*Lib models can be used to simulate the steady-state behavior [6] of the fuel cells along their complete range of operation. For instance, the polarization curve (I-V) of a fuel cell model, composed using *FuelCell*Lib, is shown in Fig. 3. The three operation areas (A, B and C) are indicated in the figure: A) fall due to the activation losses; B) fall due to the ohmic losses; and C) fall due to the mass transport at high current value.

The *FuelCell*Lib models are based in physical-chemical principles. The balances of the species (i.e., water, oxygen, protons and electrons) are enunciated, in each physical layer of the fuel cell, by means of the definition of *control volumes*.

The properties of the medium inside the control volume are considered time-dependent, but independent of the spatial coordinates. The control volumes exchange the different species with their environment through certain *control planes*. All the interactions between the control volumes are considered *transport phenomena* in *FuelCell*Lib. The physical layers of the fuel cell (i.e., the membrane and the catalytic and diffusion layers of the cathode) are modeled by decomposition into control volumes, which are connected to each other by means of transport phenomena.
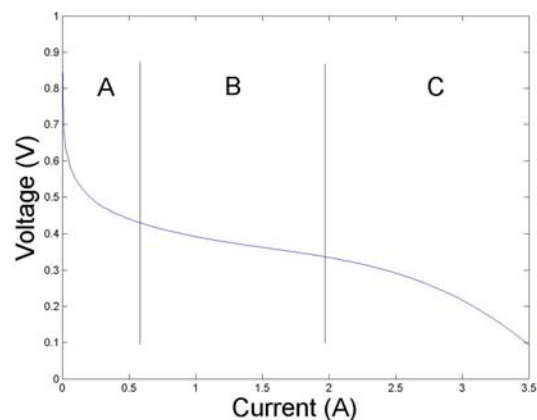

Figure 2: Species involved in the *FuelCell*Lib model of PEMFC

Figure 3: Polarization curve simulated using *FuelCell*Lib

These control volumes and transport phenomena can be modeled with different levels of detail, i.e., using different modeling hypothesis. A feature of the *FuelCell*Lib models of control volumes and transport phenomena is that they describe different modeling hypotheses. This allows the model user to select the set of hypothesis to be used in a particular simulation run.

4   Modeling hypotheses

The following considerations and approaches are taken in the model

-    The FC model is composed of the membrane, the catalytic layer of the cathode and the diffusion layer of the cathode.

-    The mixture of gases is considered an ideal gas.

-    The flow speed and the gradients of gas pressure are considered small.

-    The diffusion electrodes and the catalytic layer have a porosity and a homogeneous tortuosity, with a single pore size, which relates to the considerations of the macro-homogeneous model [9,10].

-    The electrodes, the catalytic layer and the membrane are considered isotropic and homogeneous. This is equivalent to consider that the catalyst is evenly distributed in the catalytic layer.

-    The model is one-dimensional. The variables change in the direction of the normal to the surface of the membrane and the electrodes. This direction is the x axis.

-    The temperature of each cell layer is considered uniform. Nor the Joule effect for movement of species, neither the heat obtained in the electrochemical reaction, is taken into account.

-    The movement of the gases is due to the concentration gradients and to the gas pressure in the electrodes.

-    The overvoltage of the anode is considered negligible.

-    The models are dynamic. They should be able to represent time-dependent behaviors.

-    The proton concentration inside the membrane is considered constant.

-    The crossover of oxygen in the membrane is not modeled.

-    The library user is allowed to choose among the following four mutually exclusive hypotheses:

- Pseudo-capacitance of double layer in catalyst layer.
- Pore size dependence in Knudsen diffusion.
- Electro-Osmotic drag effect in electrolyte.
- Variable electrolyte conductivity with water load.

5   Modeling equations

The equations used to model the three fundamental physical parts of the PEMFC are described in this section.

The thermodynamic open-circuit voltage is calculated [9] from Eq. (1).

$$E_{oc} = E_{ref} - 0.9 \times 10^{-9}(T - 298) + \frac{RT}{2F} \ln(\frac{p_{O_2}^{1/2} p_{H_2}}{p_{H_2O}}) \qquad (1)$$

5.1   Diffusion layer equations

- Balance of gas O_2

$$\frac{p_{O_2}}{RT}\frac{\partial \varepsilon_g}{\partial t} + \frac{\varepsilon_g}{RT}\frac{\partial p_{O_2}}{\partial t} = -\frac{dJ_{O_2}}{dx} \qquad (2)$$

where ε_g is the pore volume of the porous media. p_{O_2} and J_{O_2} are the pressure and the flow of oxygen respectively.

$$\varepsilon_g = \varepsilon_{g_0}\left[1 - \left(\frac{\chi_s}{\chi_s^{\max}}\right)^m\right] \qquad (3)$$

The pore equations are common to all physical layers. The pore volume, calculated from Eq. (3), depends on the load of water of the porous material.

$$\chi_s^{\max} = \frac{\rho^l_{H_2O}}{\rho_s}\frac{(1 - \varepsilon_s - \varepsilon_e)}{\varepsilon_s + \varepsilon_s} \qquad (4)$$

where $\chi_s^{\max}$ is the maximum load of water of the porous media. It depends on the pore volume. In the diffusion layer, the term that corresponds to the volume of the electrolyte material does not exist.

$$\varepsilon_s = 1 - \varepsilon_{g_0} - \varepsilon_e \qquad (5)$$

The total volume of any layer is equal to the sum of the pore, the solid and the electrolyte volumes, as shown in Eq. (5).

- Balance of gaseous H_2O

$$\frac{p_{H_2O}}{RT}\frac{\partial \varepsilon_g}{\partial t} + \frac{\varepsilon_g}{RT}\frac{\partial p_{H_2O}}{\partial t} = -\frac{dJ^g_{H_2O}}{dx} - \frac{\alpha_v \beta}{RT}(p_{H_2O} - p^{sat}_{H_2O}) \qquad (6)$$

where p_{H_2O} and $J^g_{H_2O}$ are the pressure and the flow of water in steam phase respectively.

The condensation and evaporation of water are taken into account in the water balance equation. The two phases are considered to be in balance, and it depends on the specific surface of the porous media.

$$p^{sat}_{H_2O} = p_0{}^{sat}_{H_2O} e^{(\frac{1}{T^{sat}_0} - \frac{1}{T})\frac{L_v M_{H_2O}}{R}} \qquad (7)$$

$$L_v = 1.73287x10^6 + 1.03001x10^{-4}T - 4.47755x10^1 T^2 + \\ + 7.6629x10^{-2}T^3 - 5.5058x10^{-5}T^4 \qquad (8)$$

The saturation pressure can be calculated from Eqs. (7-8). It essentially depends on the temperature.

- Balance of liquid H_2O

$$\frac{\rho_s}{M_{H_2O}}\frac{\partial \chi_s}{\partial t} = -\frac{dJ^l_{H_2O}}{dx} + \frac{\alpha_v \beta}{RT}(p_{H_2O} - p^{sat}_{H_2O}) \qquad (9)$$

where ρ_s is the density of the solid and M_{H_2O} is the molar mass of water. χ_s and $J^l_{H_2O}$ are the load and flux of liquid water respectively.

- Transport of gases

$$\frac{\varepsilon_g}{\tau^2}\frac{dp_i}{dx} = \sum_{k=1}^{i}\frac{RT}{p_c D_{ik}}(p_i N_k - N_i p_k) + \frac{RTJ_j}{\frac{\varepsilon_g}{\tau^2}D_j} \qquad (10)$$

the term τ represents the tortuosity of the porous material, p_c is the complete pressure and D_{ik} is the binary diffusion coefficient.

The gas flow is described by Eq. (10). It depends on the following two phenomena: the Stefan-Maxwell diffusion and the Knudsen diffusion.

$$D_{ik} = D_{ik_0}\left(\frac{p_c}{p_c{}^{ref}}\right)\left(\frac{T}{T^{ref}}\right)^{1.5} \qquad (11)$$

The binary diffusion coefficient [7] can be calculated from Eq. (11). $p_c{}^{ref}$ is the reference pressure and T^{ref} is the reference temperature used to measure the binary diffusion coefficient.

$$D_{Knudsen} = D_{Knudsen_0} \qquad (12)$$

$$D_{Knudsen} = \left(\frac{4}{3}\right)r_p\sqrt{\frac{2RT}{\pi \cdot M}} \qquad (13)$$

The Knudsen diffusion coefficient can be calculated from Eq. (12) or (13). In the first case, it is considered a constant [8]. In the second case, it depends on the pore size. The library user has to choose one of these two modeling hypotheses.

- Transport of liquid H_2O

$$J^l_{H_2O} = -\frac{\rho_s}{M_{H_2O}}D_{H_2O}\frac{d\chi_s}{dx} \qquad (14)$$

where the term D_{H_2O} corresponds to the diffusion coefficient of the liquid water in the porous media.

The flow of liquid water is produced by a gradient in the load of liquid water. This is equivalent to assume that the superficial diffusion is predominant [4].

- Electronic conduction

$$J_e = -\sigma_s \varepsilon_s \frac{dV_s}{dx} \qquad (15)$$

where V_s is the voltage of solid, J_e the electronic current and σ_s is the electronic conductivity of the solid.

The electronic conduction depends on the conductivity of the solid diffuser and the porosity of the porous media.

5.2 Catalytic layer

- Balance of gas O_2

$$\frac{p_{O_2}}{RT}\frac{\partial \varepsilon_g}{\partial t} + \frac{\varepsilon_g}{RT}\frac{\partial p_{O_2}}{\partial t} = -\frac{dJ_{O_2}}{dx} - \frac{1}{4F}\frac{dJ_e}{dx} \qquad (16)$$

The right term of the equation constitutes the oxygen balance in the catalytic layer. The last term represents the effect of the electrochemical reaction.

- Balance of gas H_2O

$$\frac{p_{H_2O}}{RT}\frac{\partial \varepsilon_g}{\partial t} + \frac{\varepsilon_g}{RT}\frac{\partial p_{H_2O}}{\partial t} = -\frac{dJ^g_{H_2O}}{dx} + \frac{1}{2F}\frac{dJ_e}{dx} - \frac{\alpha_v \beta}{RT}(p_{H_2O} - p^{sat}_{H_2O}) \qquad (17)$$

In Eq. (16) and (17), the balance of water in the catalytic layer depends on the electrochemical reaction.

- *Transport of liquid H_2O*

$$J^l{}_{H_2O} = -\frac{\rho_s}{M_{H_2O}} D_{H_2O} \frac{d\chi_s}{dx} \qquad (18)$$

Two alternative modelling hypotheses are supported. The user has to decide whether include in Eq (18) or not the electro-osmotic drag term shown in Eq. (19).

$$J^l{}_{H_2O_T} = J^l{}_{H_2O} + n_{drag} \frac{J_p}{F} \qquad (19)$$

The liquid water flow depends on: (1) the concentration gradient of liquid water; and (2) the electro-osmotic drag, which is due to the proton conduction produced inside the active-layer electrolyte. The coefficient of electro-osmotic drag can be calculated from Eq. (20). This equation is also valid for the electro-osmotic drag in the membrane.

$$n_{drag} = \frac{2.5 L_{SO_3} \varepsilon_e}{22} \qquad (20)$$

$$n_{drag} = 0.0029 L_{SO_3}{}^2 + 0.05 L_{SO_3} - 3.4 x 10^{-19} \qquad (21)$$

Eq. (20) is determined experimentally. The electro-osmotic drag mainly depends on the water content of the membrane [10]. Eq. (21) is also empiric [11]. The user needs to choose between Eq. (20) and (21).

$$L_{SO_3} = 14 \qquad (22)$$

$$L_{SO_3} = \frac{\chi_s}{\left(\frac{\rho_s}{M_m}\right) - \left(0.0126 \chi_s\right)} \qquad (23)$$

The electro-osmotic drag coefficient depends on the L_{SO_3} term. This term is a function of the load of water in the electrolyte. Two possible expressions are considered in the library. The first one is the constant value shown in Eq. (22), which has been calculated from saturated water vapor at 30ºC. The second one is the expression shown in Eq. (23), which takes into account the dependence with respect to the water load.

- Protonic conduction

$$J_p = -K_p \varepsilon_m \frac{dV_e}{dx} \qquad (24)$$

where V_e represents the electrolyte voltage , J_p the protonic current, K_p the protonic conductivity and ε_m the electrolyte volume.

The protonic conduction is produced by a voltage gradient in the protonic conductive material.

- *Electrochemical reaction*

$$\nabla J_e = a_{act} i_0 \left[\frac{p_{O_2}}{p^0{}_{O_2}} \exp\left(\frac{\alpha n F}{RT} \eta_D\right) - \exp\left(\frac{-1(1-\alpha)nF}{RT} \eta_D\right) \right] \qquad (25)$$

where i_0 is the exchange current in open circuit, a_{act} is the specific active surface in catalytic layer , $p^0{}_{O_2}$ is the reference partial pressure of oxygen, α is the transfer coefficient of charge in cathode y η_D is the overvoltage between the solid and electrolyte.

Eq. (25) is the Butler-Bolmer expression of the electrochemical reaction. The anode contribution can be neglected [1,4,5].

The model allows the user to choose between Ec. (25) or (26). The pseudo-capacitance is considered in Eq. (26) [1].

$$\nabla J_{T_e} = \nabla J_e + C_{dl} \frac{\partial \eta}{\partial t} \qquad (26)$$

The term ∇J_e in Eq. (26) is calculated from Eq. (25). C_{dl} is the capacitance of the double layer between the solid and the electrolyte.

The characteristics of the macro-homogeneous model lead to an underestimation of the overvoltage effect associated to the defect of mass in high current densities. To characterize this phenomenon we introduce in the model Eq. (27), (28) and (29).

$$i_o = i^{ref}{}_o \left(1 - \frac{J_e}{J_l}\right) \qquad (27)$$

$$J_l = \left(\frac{p_{O_2}}{p^0{}_{O_2}}\right) J_{\lim} \qquad (28)$$

$$J_{\lim} = \frac{AD_{effO_2}}{\delta} \qquad (29)$$

where A is the active surface of the catalytic layer. In the macro-homogeneous model, δ defines the thickness of the catalytic layer [12].

The balance equations of the liquid water, the transport of gases and the electronic conduction are similar to the correspondent equations of the diffusion layer.

5.3 Membrane

- *Balance of gas H_2O*

$$\frac{p_{H_2O}}{RT}\frac{\partial \varepsilon_g}{\partial t} + \frac{\varepsilon_g}{RT}\frac{\partial p_{H_2O}}{\partial t} = -\frac{dJ^g_{H_2O}}{dx} - \frac{\alpha_v \beta}{RT}(p_{H_2O} - p^{sat}_{H_2O}) \qquad (30)$$

- *Balance of liquid H_2O*

$$\frac{\rho_s}{M_{H_2O}}\frac{\partial \chi_s}{\partial t} = -\frac{dJ^l_{H_2O}}{dx} + \frac{\alpha_v \beta}{RT}(p_{H_2O} - p^{sat}_{H_2O}) \qquad (31)$$

- *Transport of liquid H_2O*

$$J^l_{H_2O} = -\frac{\rho_s}{M_{H_2O}}D_{H_2O}\frac{d\chi_s}{dx} + n_{drag}\frac{J_p}{F} \qquad (32)$$

- *Transport of gas H_2O*

$$J^l_{H_2O} = -\frac{\tau^2 RT}{\varepsilon_g}D^g_{H_2O}\frac{dp_{H_2O}}{dx} \qquad (33)$$

- *Protonic conduction*

$$J_p = -K_p \varepsilon_m \frac{dV_e}{dx} \qquad (34)$$

$$k_p = k_{p0} \qquad (35)$$

$$k_p = (0.005139\, L_{SO_3} - 0.00326)e^{1268\left(\frac{1}{303} - \frac{1}{273+T}\right)} \qquad (36)$$

The model supports two alternative hypotheses. The first one is to consider constant conductivity, as shown in Eq. (35). The second one is to consider the effect of the water load on the conductivity of the electrolyte [10], as shown in Eq. (36).

6   Library structure

The hierarchical structure of *FuelCell*Lib library is represented in Fig. 4. In addition, *FuelCell*Lib includes models for experimenting with the fuel-cells. For instance, it contains the model of a binary pseudo-random signal generator of electric load. These components are used to perform for dynamic analysis of the fuel-cell. For instance, the voltage of a FC, which has been connected to a step-signal generator of electric load, is shown in Fig.5.

The electric parts of *FuelCell*Lib models can be connected to the models of the *Electrical* package of the Standard Modelica library. This feature allows combining the use of *FuelCell*Lib and other Modelica libraries.

The structure of the library allows the user to choose among different modelling hypotheses. This selection is performed by setting the value of certain model parameters. This structure facilitates extending the library with new alternative hypotheses, and also comparing the dynamic behavior of the models built by using the different hypotheses.

Figure 4: Packages and models of *FuelCell*Lib

Figure 5: Effect of step load in the cell voltage. Dynamic simulation.

Four sets of alternative hypotheses are supported by *FuelCell*Lib. Different hypotheses leads to different dynamic behaviour of the model (see Figs. 6 and 7).

Two case studies are presented in this work: (1) the simulation of two physical layers (membrane and active layer); and (2) the simulation of the three physical layers (membrane, active and diffusion layer). The results are discussed in the next section.

7   Validation of library

PEMFCs and DMFCs are developed in the Renewable Energy Laboratory of the Industrial Automatic Institute (IAI) of CSIC (see Fig. 8). These fuel-cells have been employed to carry out the experimental validation of the *FuelCell*Lib library.

The simulation results obtained using *FuelCell*Lib agree with the theoretical and the experimental data. A simulated polarization curve, obtained using *FuelCell*Lib, and experimental data, measured from a PEMFC manufactured in the I.A.I, are shown in Fig. 9.
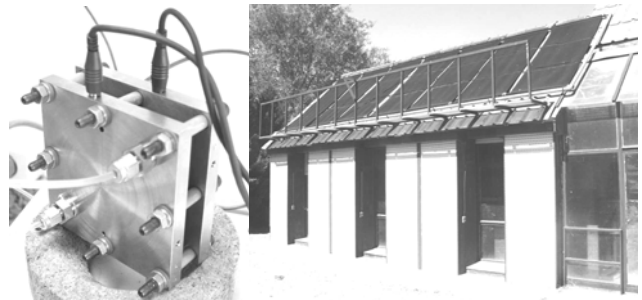
Figure 8: Fuel-cell (left) developed in the Renewable Energy Laboratory of the Industrial Automatic Institute (IAI) of CSIC, Madrid, Spain (right)
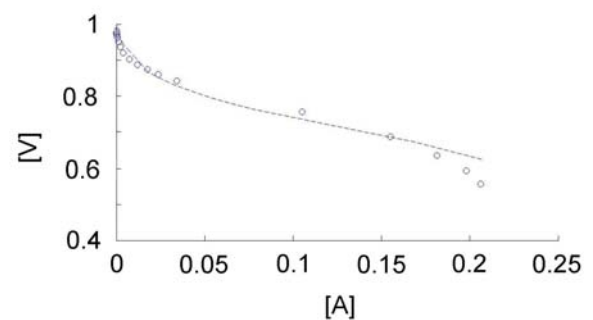
Figure 9: Experimental and simulated polarization curve, exp. (o), model (- -), ($2x10^5$ Pa of O_2, T= 340ºK).

Simulation results using *FuelCell*Lib are shown in Fig. 10. They can be compared with the results obtained using the model of K.Broka [5] (see Fig. 11). Both results predict the fall of the oxygen concentration along the catalytic layer, and how the fall is bigger as the current increases.

Simulation results obtained using *FuelCell*Lib are compared in Fig. 12 with the experimental data presented by J. Larminie [13]. Both predict the effect of the Tafel slope on the polarization curve (see Fig.12).

The simulated voltage of the fuel-cell, obtained in response to a step change in the load, is shown in Fig. 5. It agrees with the experimental data provided by J. Larminie [13].

In addition, *FuelCell*Lib can be used to predict phenomena which can not be measured experimentally. For instance, the effect of flooding of the cathode, (see Fig. 13), the water load in the catalytic layer and the membrane. The production of water in the catalytic layer, associated to the diffusion in the catalytic layer and the membrane, is shown in Fig. 13.
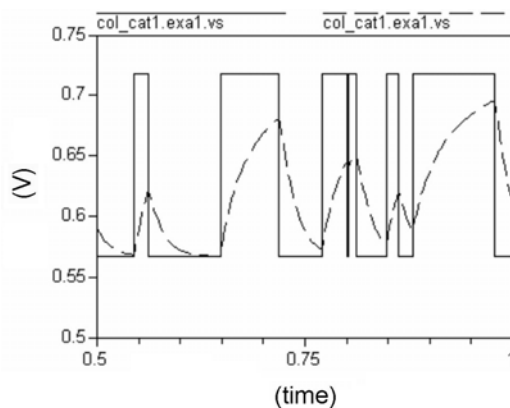
Figure 6: Dynamic simulation of voltaje of FC with a psuedo-capacitance hypothesis dependence (- - -) and without psuedo-capacitance hypothesis dependence (___).
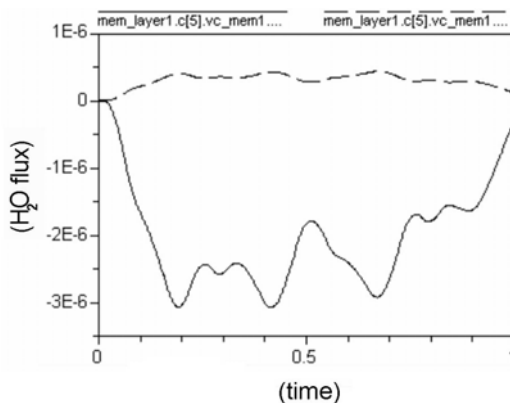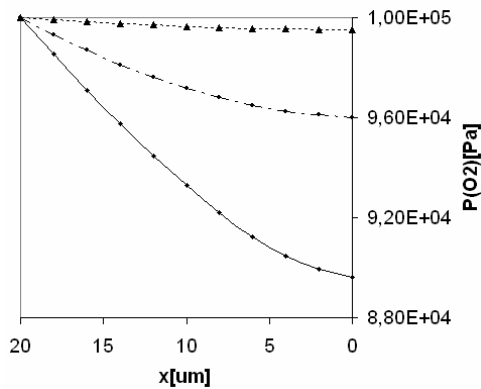
Figure 7: Dynamic simulation of flux of water in membrane with electro-osmotic drag hypothesis dependence (- - -) and without electro-osmotic drag hypothesis dependence (___).

Figure 10: Pressure of oxygen along the catalyst layer with three different current density, 12mA/cm2 (. . .), 90mA/cm2 (- - -), 230mA/cm2 (___); (2x10^5 Pa of O$_2$, 340ºK).
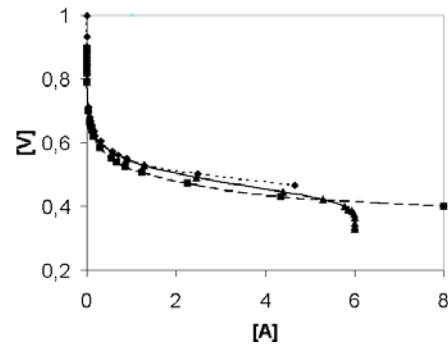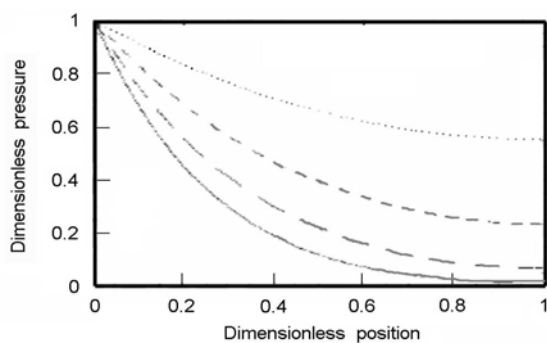

Figure 11: Oxygen pressure in the cathode in x axis in K.Broka model, (.....)250, (- - - -) 500, (_ _ _) and 1000 (___) mA /cm^2.
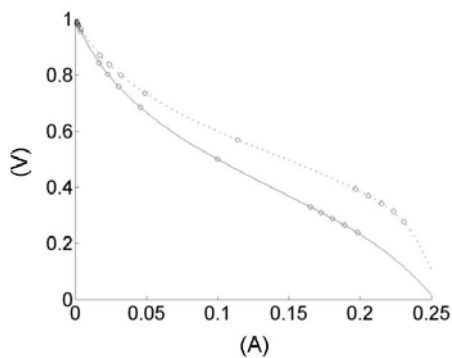

Figure 12: Influence of Tafel slope in polarization curve (I-V) in the library (---150mv),(___200mv).
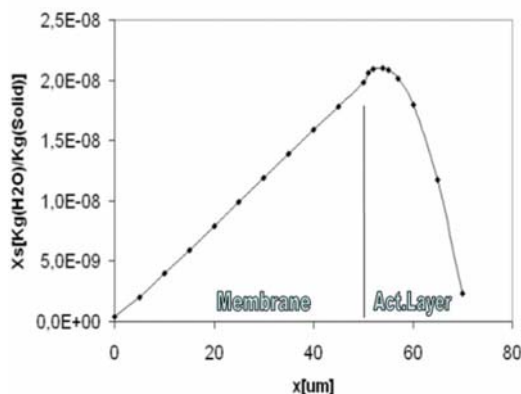

Figure 13: Water load in cathode along the x axis.

Figure 14: Effect of limit current in polarization curve (. . .) no limit current dependence, (- - -) limit current with no pressure dependence, (___) limit current with pressure dependence.

The effect of the limit current on the polarization curve, simulated using *FuelCell*Lib is shown in Fig. 14.

The simulated polarization curves (see Fig.3, 9, 12, 14) are obtained by reaching a stationary value in the dynamic simulation of the models.

8   Conclusions

*FuelCell*Lib has demonstrated to be useful for improving the understanding of the phenomena involved in the fuel-cell operation. The object-oriented design of the library facilitates the extension, modification and reuse of its code. In addition, the library structure facilitates introducing new modelling hypotheses and comparing the results obtained by using these different hypotheses. The code of the library models is easy to understand by other developers.

9   Future works

Future releases of the library will support the following capabilities: (1) 2D and 3D models, which allow to represent in a detailed way the fluid-dynamics phenomena; (2) new modeling hypotheses that describe the electro-catalytic phenomena with higher level of detail, such as the thin film or agglomerate models; and (3) new models to simulate DMFC (direct methanol fuel cell) and SOFC (solid oxide fuel cell).

Finally, we will be able to obtain a greater quantity of experimental data of the FCs, to achieve a more detailed experimental validation of the library.

References

[1]   M.Ceraolo, C.Miulli, A.Pozio, Modeling static and dynamic behaviour of PEMFC on the basis of electro-chemical description, J. Power Sources 113 (2003).

[2]   A.Kumar, R.Reddy, Effect of channel dimensions and shapes in the flow-field distributor on performance of PEMFC, J. Power Sources 113 (2003).

[3]   W.D.Steinmann, P.Treffinger, Simulation of Fuel Cell Powered Drive Trains, Modelica WorkShop 2000 Procedings.

[4]   D.Bevers, M.Wöhr, K.Yasuda, K.Oguro, Simulation of polymer electrolyte fuel cell electrode.J.Appl. Electrochem.27 (1997).

[5]   K.Broka, P.Ekdunge, Modelling the PEM fuel cell cathode, J.Appl. Electrochem.27 (1997).

[6]   J.Larminie, A.Dicks, Fuel Cell Systems Explained, Wiley 2000.

[7]   A.A.Kulikovsky, Fuel Cells 2001,1(2).

[8]   V.Gurau, H.Liu, S.Kakac,AIChE J.2000 46(10).

[9]   D.M.Bernardi, M.W.Verbrugge, J. electrochem. Soc. 139,9 (1992).

[10] T.E.Springer, T.A.Zawodzinsky, J.Electrochem.Soc. 138 (1991).

[11] S.Dutta, S.Shimpalee, J.Appl.Electrochem. (2000), 30(2).

[12] D.B.Genevey, Thesis, F.V.P.I. (2001).

[13] J. Larminie, A.Dicks, Fuel Cell System Explained, Wiley (2000).